

Factorized Latent Dynamics for Video JEPA: An Empirical Study of Auxiliary Objectives

Santosh Premi Adhikari

Abstract

*Joint-Embedding Predictive Architectures (JEPA) are a promising framework for self-supervised video representation learning, yet the behavior of auxiliary objectives in small-scale Video-JEPA training is not well characterized. We report a small-scale empirical study of **18 auxiliary objective variants** for Video-JEPA across two pretraining regimes: single-dataset (UCF-101) and mixed-dataset (UCF-101 + Something-Something V2 + ImageNet-100). We evaluate frozen representations on three complementary benchmarks: Diving-48 (fine-grained motion), Something-Something V2 (temporal reasoning), and ImageNet-100 (appearance).*

*Our experiments suggest that many auxiliary objectives exhibit **capacity trade-offs**: gains on one downstream capability often coincide with degradation on another. We then study **FWM-HW-LD** (Factorized World-Model with Hard-Region-Weighted Latent Dynamics), a training-time objective that separates the latent representation into appearance and dynamics subspaces and applies hard-region weighting to both JEPA prediction errors and latent dynamics errors. In our mixed-dataset setting, FWM-HW-LD improves ImageNet-100 by **+5.92** and SSv2 by **+3.21** percentage points relative to the reference baseline, while remaining within **0.30** percentage points on Diving-48. These results indicate that latent factorization is a useful direction for studying auxiliary-objective trade-offs in Video-JEPA.*

Code: <https://github.com/santoshpremi/Factorized-Latent-Dynamics-for-Video-JEPA-An-Empirical-Study-of-Auxiliary-Objectives>

1. Introduction

Video understanding requires models to capture both static appearance (what objects look like) and temporal dynamics (how they move and interact). The Video Joint-Embedding Predictive Architecture (V-JEPA) [3, 6] addresses this through masked video modeling in a learned latent space, predicting embeddings of masked spatiotemporal regions from visible context without pixel-level re-

construction. This approach is theoretically motivated by the JEPA framework [2, 29], which argues that learning predictive world models in abstract latent space avoids the wasteful task of modeling unpredictable pixel-level details, in contrast to pixel-reconstruction methods such as MAE [24, 45].

While V-JEPA has demonstrated strong results on video understanding benchmarks [6], the standard training objective—predicting teacher encoder embeddings with a latent prediction loss—does not explicitly isolate fine-grained temporal dynamics from appearance information. This can matter for downstream tasks such as Diving-48 [30] and Something-Something V2 [19], where temporal ordering and motion cues are central.

Recent theory on JEPA with auxiliary tasks argues that auxiliary signals can determine which distinctions a representation must preserve [52]. This motivates our empirical question: under a fixed small-scale Video-JEPA budget, which auxiliary objectives help transfer, and which introduce trade-offs across motion- and appearance-sensitive evaluations?

We conduct an empirical study across **18 auxiliary objective variants**, organized into six categories:

1. **Kinematic Regularization** — L1, Huber, acceleration, split-channel, and annealed penalties on temporal differences.
2. **Motion-Guided Masking** — biasing mask sampling toward high-motion regions.
3. **Anti-Collapse Regularization (SIGReg)** — enforcing Gaussian-distributed latent embeddings [33].
4. **Physics-Inspired Dynamics** — Hamiltonian and velocity-gated priors on latent evolution.
5. **Latent Dynamics Prediction** — predicting temporal differences in latent space (Delta-JEPA, LD-JEPA, Spectral-JEPA, LTC-JEPA).
6. **Factorized Latent Objectives** — structurally separating appearance and dynamics subspaces during training (FWM-JEPA, FWM-HW-LD).

Our contributions are as follows:

1. A small-scale empirical study of V-JEPA auxiliary objectives, spanning 18 variants across three benchmarks

- under a shared training budget.
- Evidence for **capacity trade-offs**: many auxiliary objectives improve one downstream capability while degrading another in the same frozen encoder.
 - FWM-HW-LD**: a factorized latent-dynamics training objective that gives the most balanced result in our mixed-dataset sweep, improving ImageNet-100 (+5.92 pp) and SSv2 (+3.21 pp) while remaining close to the reference baseline on Diving-48 (−0.30 pp).
 - Practical observations and failure cases that may guide future, larger-scale studies of auxiliary objectives for Video-JEPA.

2. Related Work

Self-supervised image representation learning. Self-supervised pretext tasks for images include context prediction [14], jigsaw puzzles [36], and contrastive instance discrimination [11, 12, 23]. Cluster-based approaches such as SwAV [8], distillation methods such as BYOL [20] and DINO [9], redundancy-reduction methods such as Barlow Twins [53], and information-theoretic methods such as DIM [26] and CPC [37] have all advanced the state of the art. More recently, masked image modeling methods including BEiT [4], SimMIM [49], and MAE [24] have demonstrated that pixel reconstruction with high masking ratios learns strong visual features.

Joint-embedding predictive architectures. JEPA [29] predicts latent representations of unseen content from observed content rather than reconstructing pixels. I-JEPA [2] demonstrated this paradigm at image scale, while V-JEPA [6] extended it to video. V-JEPA 2 [3] scales the approach with larger backbones and curated video data, and V-JEPA 2.1 [35] introduces dense/context prediction, deep self-supervision, multi-modal tokenizers, and further scaling to improve dense video features while preserving global recognition. This recent work is important for our study because it shows that changing where and how the V-JEPA prediction loss is applied can improve one representation property while stressing another. Recent theory on JEPA auxiliary tasks [52] likewise suggests that auxiliary signals influence which distinctions are preserved in the latent representation. Closely related is LeJEPA [33], which proposes SIGReg, a sketched-isotropic-Gaussian regularization that prevents collapse without requiring an EMA target. Our work is orthogonal: we study which auxiliary objectives help small-scale V-JEPA learn motion-discriminative representations, on top of the underlying joint-embedding objective.

Self-supervised video representation learning. Early video SSL methods exploited temporal structure as a free supervisory signal: shuffle-and-learn [34], clip order prediction [50], motion segmentation from optical flow [39],

and cycle-contrastive prediction [22, 28]. Contrastive video methods such as VideoMoCo [38], BraVe [40], and CBT [43] extend instance discrimination to temporally augmented clips. The current state of the art is dominated by masked video modeling: VideoMAE [45, 48], ST-MAE [18], and Siamese MAE [21] reconstruct masked tubelets, while V-JEPA [6] predicts latent embeddings. Multi-view objectives [44, 51] provide complementary signals.

Video architectures and benchmarks. We adopt ViT [15, 47] as the encoder backbone, following V-JEPA. Alternative video backbones include I3D [10], R(2+1)D [46], SlowFast [17], MViT [16], ViViT [1], TimeSformer [7], and Video Swin [31]. Standard evaluation benchmarks include UCF-101 [42] (general action recognition), Diving-48 [30] (fine-grained motion without representation bias), Something-Something V2 [19] (temporal reasoning), EPIC-KITCHENS [13] (egocentric), and Kinetics [10]. ImageNet [41] provides image-level evaluation. Bardes *et al.* [5] introduce variance-invariance-covariance regularization to prevent collapse.

Latent-space factorization. Disentangled representation learning has been explored extensively in VAE-based frameworks [25, 27] and contrastive settings [44]. We apply factorization specifically to the JEPA encoder-predictor architecture, structurally separating appearance-invariant and dynamics-sensitive channel groups within the same encoder output, and combine it with hard-region weighted latent dynamics prediction. This is a training-time channel partition of V-JEPA features, not an object-centric, action-factorized, or generative world model.

3. Method

3.1. V-JEPA Baseline

The V-JEPA [6] architecture consists of a **student encoder** f_θ (ViT-Base [15], 86M parameters, patch 16×16 , tubelet 2, RoPE positional encoding) encoding visible spatiotemporal patches from 16-frame clips into latent representations $z \in \mathbb{R}^{T \times H \times W \times D}$, a **teacher encoder** $f_{\hat{\theta}}$ (EMA of student weights, following BYOL [20] and DINO [9]) producing targets h , and a **predictor** g_ϕ (8-layer Transformer, embed dim 256, 8 heads) predicting masked region embeddings from visible context. Following the original V-JEPA implementation [6], the training objective is a distance-weighted ℓ_1 loss:

$$\mathcal{L}_{\text{JEPA}} = \mathbb{E} [\| \hat{z} - \text{sg}(h) \|_1] \quad (1)$$

where $\text{sg}(\cdot)$ denotes stop-gradient on the teacher output. Distance weighting down-scales the loss contribution of spatially distant mask regions, as in the original V-JEPA code.

V-JEPA latent prediction

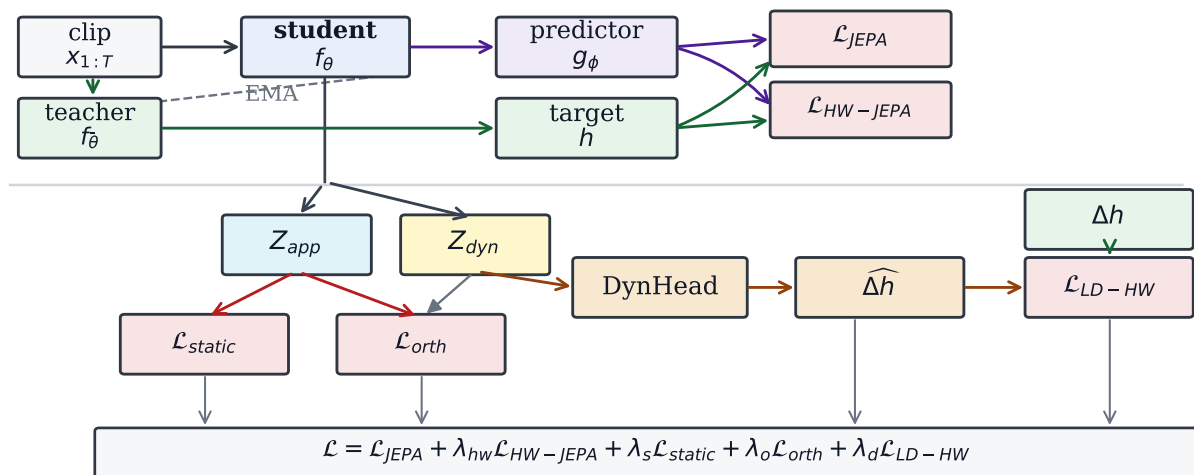


Figure 1. **FWM-HW-LD training objective overview.** The standard V-JEPA latent prediction path is retained. During training, the student encoder output is additionally partitioned into appearance (Z_{app}) and dynamics (Z_{dyn}) subspaces. Hard-region weighting is applied to the JEPA prediction error ($\mathcal{L}_{HW-JEPA}$) and, when latent dynamics is enabled, to the latent dynamics error (\mathcal{L}_{LD-HW}). Additional FWM losses encourage temporal stability in Z_{app} and decorrelation between Z_{app} and Z_{dyn} .

3.2. Kinematic Regularization

Five variants penalize temporal differences in encoder embeddings. In our UCF-101 kinematic runs, EMA is disabled, so this term is applied to the trainable encoder output rather than a frozen teacher target:

Kinematic-L1. L1 penalty on first-order temporal differences:

$$\mathcal{L}_{kin} = \lambda \cdot \mathbb{E} \left[|h^{(t+1)} - h^{(t)}| \right] \quad (2)$$

Kinematic-Huber. Replaces L1 with Huber loss for robustness to outliers.

Kinematic-Accel. Penalizes second-order temporal differences:

$$\mathcal{L}_{accel} = \lambda \cdot \mathbb{E} \left[|h^{(t+2)} - 2h^{(t+1)} + h^{(t)}| \right] \quad (3)$$

Kinematic-Split. Applies the acceleration-style kinematic penalty only to the first half of the channels, leaving the remaining channels unconstrained.

Kinematic-Anneal. Cosine annealing of λ throughout training.

3.3. Motion-Guided Masking

Standard V-JEPA masks random spatiotemporal tubes, following the masking strategies of MAE [24] and VideoMAE [45]. We bias mask center sampling toward high-motion regions, drawing inspiration from motion-driven SSL [39]:

$$P(\text{center}) \propto \exp\left(\alpha \cdot \|\text{frame}^{(t+1)} - \text{frame}^{(t)}\|\right) \quad (4)$$

With probability 0.1 we fall back to uniform random sampling. This modifies the training data distribution without adding any auxiliary loss term.

3.4. SIGReg

Following Maes *et al.* [33], we project latent embeddings onto random unit vectors and apply normality testing. Evaluated with standard EMA teacher (**SIGReg**) and without EMA (**SIGReg-no-EMA**).

3.5. Physics-Inspired Dynamics

Hamiltonian-JEPA. Decomposes the latent embedding into position q and momentum p channels. A learned Hamiltonian $H(q, p)$ enforces energy-conserving dynamics via Hamilton's equations.

Velocity-Gated JEPA (VelGate). Applies kinematic regularization selectively to low-velocity (background) tokens only.

3.6. Latent Dynamics Prediction

Delta-JEPA. Aligns student temporal differences with teacher temporal differences:

$$\mathcal{L}_\Delta = \|z^{(t+1)} - z^{(t)} - \text{sg}(h^{(t+1)} - h^{(t)})\|_1 \quad (5)$$

LD-JEPA (Latent Dynamics). A dedicated MLP dynamics head predicts the teacher's temporal difference from the student's representation:

$$\mathcal{L}_{LD} = \|\text{DynHead}(z^{(t)}) - \text{sg}(h^{(t+1)} - h^{(t)})\|_1 \quad (6)$$

Spectral-JEPA. Applies FFT along the temporal dimension and minimizes L1 on frequency-weighted spectral coefficients.

LTC-JEPA (Latent Temporal Contrastive). Margin-based contrastive loss ensuring $z^{(t)}$ is closer to $h^{(t)}$ than to $h^{(t+1)}$ in cosine similarity, in the spirit of contrastive video representation learning [22, 28, 40].

3.7. Factorized World-Model JEPA (FWM-JEPA)

FWM-JEPA structurally separates the encoder’s D -dimensional output into two subspaces:

- Z_{app} (first $D/2$ channels): Appearance subspace, encouraged to be temporally invariant.
- Z_{dyn} (remaining $D/2$ channels): Dynamics subspace, free to capture temporal variation.

$$\mathcal{L}_{\text{static}} = \mathbb{E} \left[|Z_{\text{app}}^{(t+1)} - Z_{\text{app}}^{(t)}| \right] \quad (7)$$

$$\mathcal{L}_{\text{orth}} = \frac{1}{N} \|C_{Z_{\text{app}}}^T C_{Z_{\text{dyn}}}\|_F^2 \quad (8)$$

where C denotes centered features.

3.8. FWM-HW-LD: Factorized Latent-Dynamics Training Objective

FWM-HW-LD is a training objective rather than a new inference-time architecture. It combines four loss components:

1. **Factorization (FWM):** Z_{app} and Z_{dyn} are encouraged to carry less redundant information via $\mathcal{L}_{\text{static}}$ and $\mathcal{L}_{\text{orth}}$.
2. **Hard-Weighted JEPA (HW-JEPA):** the standard JEPA prediction error is reweighted toward high-error target tokens.
3. **Latent Dynamics (LD):** a dynamics head predicts $h^{(t+1)} - h^{(t)}$ from only Z_{dyn} , encouraging this subspace to carry temporally predictive information during training.
4. **Hard-Weighted Latent Dynamics (LD-HW):** the latent dynamics error is also reweighted toward high-error temporal tokens:

$$w_i = \frac{\exp(e_i/\tau)}{\sum_j \exp(e_j/\tau)} \cdot N_{\text{tokens}} \quad (9)$$

$$\mathcal{L}_{\text{HW-JEPA}} = \frac{1}{N} \sum_i w_i^{\text{jepa}} \cdot \|\hat{z}_i - h_i\|_1 \quad (10)$$

$$\mathcal{L}_{\text{LD-HW}} = \frac{1}{N} \sum_i w_i^{\text{ld}} \cdot \|\hat{\Delta}_i - \Delta h_i\|_1 \quad (11)$$

The total loss for FWM-HW-LD is:

$$\mathcal{L} = \mathcal{L}_{\text{JEPA}} + \lambda_{hw} \mathcal{L}_{\text{HW-JEPA}} + \lambda_s \mathcal{L}_{\text{static}} + \lambda_o \mathcal{L}_{\text{orth}} + \lambda_d \mathcal{L}_{\text{LD-HW}} \quad (12)$$

All dynamics prediction occurs in latent space rather than pixel space, following the central design motivation of JEPA-style feature prediction. At evaluation time, we use the frozen student encoder as in the baseline; the auxiliary dynamics head is only a training-time scaffold. The objective is illustrated in Figure 1. The term “factorized world-model” in this report should be read narrowly: it refers to a split of the V-JEPA latent channels into appearance-regularized and dynamics-regularized groups during training, not to a separately learned object-factorized simulator or action-conditioned planner.

3.9. Additional Variants Used in the Tables

Future-Predictive masking. Uses the V-JEPA objective with temporally constrained complementary masks (`full_complement=true`, `max_temporal_keep=0.5`) so prediction emphasizes temporally separated target regions.

Motion-Future. Combines Future-Predictive masking with Motion-Guided sampling (`motion_guided=true`, `strength=2.0`).

AMG-JEPA. Aggressive Motion-Guided masking uses stronger motion bias (`strength=5.0`) and no random fallback (`motion_guided_random_rate=0.0`).

AC-JEPA and FAC-JEPA. AC-JEPA predicts per-token RGB patch-mean frame differences from student features using an L1 loss. FAC-JEPA combines AC-JEPA with FWM; in that case the action head receives only Z_{dyn} .

Combination rows. AC+HW adds HW-JEPA to AC-JEPA. Combo combines Delta-JEPA with HW-JEPA and aggressive motion-guided masking. HW-LD combines HW-JEPA with hard-weighted latent dynamics but without FWM factorization.

4. Experimental Setup

4.1. Pretraining Configuration

We pretrain ViT-Base [15] encoders with AdamW [32] on either UCF-101 [42] alone or a balanced mixture of UCF-101, SSv2 [19], and ImageNet-100 [41]. Methods share architecture, data mixture, schedule, and optimizer settings (Table 1); no per-method tuning is performed. Mixed-dataset deltas are reported as percentage-point changes against the complete three-benchmark reference baseline available for the study.

Table 3. Top-1 accuracy (%) with UCF-101 pretraining. \uparrow/\downarrow denote percentage-point changes relative to baseline. **Bold** = best. Motion-Guided improves all reported metrics in this table.

Method	D-48	IN-100	SSv2	Univ.
Baseline V-JEPA	8.38	12.02	2.07	—
Motion-Guided	8.68\uparrow	12.16\uparrow	3.45\uparrow	Yes
Kin.-L1 ($\lambda=1.0$)	5.58 \downarrow	13.64 \uparrow	—	No
Kin.-L1 ($\lambda=0.1$)	5.84 \downarrow	13.66 \uparrow	3.07 \uparrow	No
Kin.-Accel	5.79 \downarrow	13.74 \uparrow	3.18 \uparrow	No
Kin.-Huber	5.99 \downarrow	—	—	No
Kin.-Split	5.48 \downarrow	13.58 \uparrow	—	No
Kin.-Anneal	5.63 \downarrow	—	—	No
SIGReg	6.29 \downarrow	—	—	No
SIGReg-no-EMA	5.99 \downarrow	—	—	No
Hamiltonian	6.04 \downarrow	—	—	No
VelGate	5.84 \downarrow	—	—	No
Future-Predictive	7.11 \downarrow	—	—	No
Motion-Future	6.45 \downarrow	—	—	No

Table 1. Pretraining configuration for both experimental regimes.

Component	Single-Dataset	Mixed-Dataset
Backbone	ViT-Base (86M), patch 16×16 , tubelet 2, RoPE	
Predictor	8-layer Transformer, embed dim 256, 8 heads	
Input	16 frames, frame stride 2, crop 224×224	
Precision	bfloat16	
Data	UCF-101 (13K)	UCF + SSv2 + IN-100
Data weights	— 20% / 60% / 20%	
Schedule	100 epochs, 300 iter/epoch	
Batch size	8×4 GPUs = 32	
Optimizer	AdamW, lr = 6×10^{-4} , wd = 0.04	
LR warmup	1 epoch, $10^{-4} \rightarrow 6 \times 10^{-4}$ (cosine)	
EMA momentum	0.99925 (constant)	
Loss	ℓ_1 (loss_exp = 1.0), distance-weighted	
Hardware	$4 \times$ NVIDIA A100 40 GB, ~ 7 h/run	

4.2. Evaluation Protocol

We follow the frozen-encoder evaluation protocol of V-JEPA [3, 6], training attentive or linear probes on three complementary downstream benchmarks (Table 2). Diving-48 [30] measures fine-grained motion understanding without representation bias, SSv2 [19] measures temporal reasoning, and ImageNet-100 [41] measures appearance recognition.

Table 2. Evaluation benchmarks and probe configuration.

Benchmark	Task	Cls.	Ep.	Probe
Diving-48	Fine-grained diving	48	50	Attentive
ImageNet-100	Object/scene recog.	100	50	Linear
SSv2	Temporal reasoning	174	50	Attentive

5. Results

5.1. Single-Dataset Results (UCF-101 Pretraining)

Table 3 presents results from 12 methods pretrained on UCF-101 only.

Finding 1: Motion-Guided Masking improves all reported metrics in the UCF-101 setting (+0.30 pp D-48, +0.14 pp

IN-100, +1.38 pp SSv2). Kinematic variants degrade D-48 by 2.5–2.9 points while improving IN-100 by 1.5–1.7 points, suggesting a motion–appearance trade-off under this training budget.

5.2. Mixed-Dataset Results

Table 4 presents the complete mixed-dataset results.

Finding 2: FWM-HW-LD achieves +5.92 percentage points on ImageNet-100 and +3.21 percentage points on SSv2 while remaining close to the Diving-48 reference baseline (−0.30 percentage points). In this mixed-dataset sweep, it gives the most balanced result among the tested variants, but this should be interpreted as a single-seed empirical signal rather than a statistically established ranking.

Implementation note. The HW coefficient affects two terms when LD is enabled: it adds $\mathcal{L}_{\text{HW-JEPA}}$ on the standard prediction error, and it also hard-weights the latent dynamics error in $\mathcal{L}_{\text{LD-HW}}$.

Finding 3: LD-JEPA achieves +5.02 pp on SSv2, the largest temporal reasoning gain in the table, suggesting that latent dynamics prediction can help temporal reasoning in this setup even when it hurts other benchmarks.

Finding 4: Many auxiliary objectives coincide with substantial degradation—10 of 14 methods lose >5 points on ImageNet-100, and pixel-prediction objectives (AC-JEPA, FAC-JEPA) are particularly weak in this setup (−13 to −16 pp).

5.3. Ablation: Components of FWM-HW-LD

The ablation (Table 5) suggests that the components interact non-additively. LD alone boosts SSv2 (+5.02) but hurts ImageNet and Diving-48. FWM alone boosts ImageNet (+1.88) but hurts SSv2 and Diving-48. FWM+LD without hard weighting performs poorly on ImageNet (−10.14). The full FWM-HW-LD combination gives the most balanced result in this ablation, consistent with the hypothesis that FWM, LD, and HW are complementary under this training budget.

5.4. Synthetic Motion Discrimination

The +40–45 point improvement (Table 6) confirms kinematic regularization encodes strong temporal structure, but this structure suits synthetic primitives rather than real-world fine-grained motion.

6. Analysis

6.1. Capacity Trade-Offs in a Shared Latent Space

The encoder produces a fixed 768-dimensional embedding that must simultaneously encode (1) what objects are present and (2) how they move. In our experiments, auxiliary objectives that emphasize temporal structure often coincide with weaker appearance discrimination. This is evi-

Table 4. Top-1 accuracy (%) with mixed-dataset pretraining (UCF-101 + SSv2 + ImageNet-100). Δ is the percentage-point change relative to the complete reference baseline used in this study. **Green** = gains. **Red** = losses >5 points.

Method	Diving-48	Δ	ImageNet-100	Δ	SSv2	Δ
Baseline	8.68	—	24.86	—	8.39	—
FWM-HW-LD	8.38	-0.30	30.78	+5.92	11.60	+3.21
LD-JEPA	6.95	-1.73	22.80	-2.06	13.41	+5.02
FWM-JEPA	7.16	-1.52	26.74	+1.88	7.00	-1.39
AC+HW-JEPA	9.39	+0.71	18.14	-6.72	4.88	-3.51
AMG-JEPA	5.89	-2.79	23.54	-1.32	7.78	-0.61
HW-JEPA	8.98	+0.30	18.46	-6.40	6.30	-2.09
HW-LD-JEPA	7.92	-0.76	19.78	-5.08	5.41	-2.98
FWM-LD-JEPA	6.40	-2.28	14.72	-10.14	7.63	-0.76
Combo	7.16	-1.52	18.60	-6.26	5.00	-3.39
Delta-JEPA	7.41	-1.27	16.76	-8.10	3.80	-4.59
AC-JEPA	8.38	-0.30	11.70	-13.16	4.21	-4.18
FAC-JEPA	8.38	-0.30	8.58	-16.28	3.08	-5.31
LTC-JEPA	7.77	-0.91	11.34	-13.52	4.32	-4.07
Spectral-JEPA	5.69	-2.99	12.62	-12.24	3.37	-5.02

Capacity Trade-offs: Mixed-Dataset Results (Δ vs. Baseline)

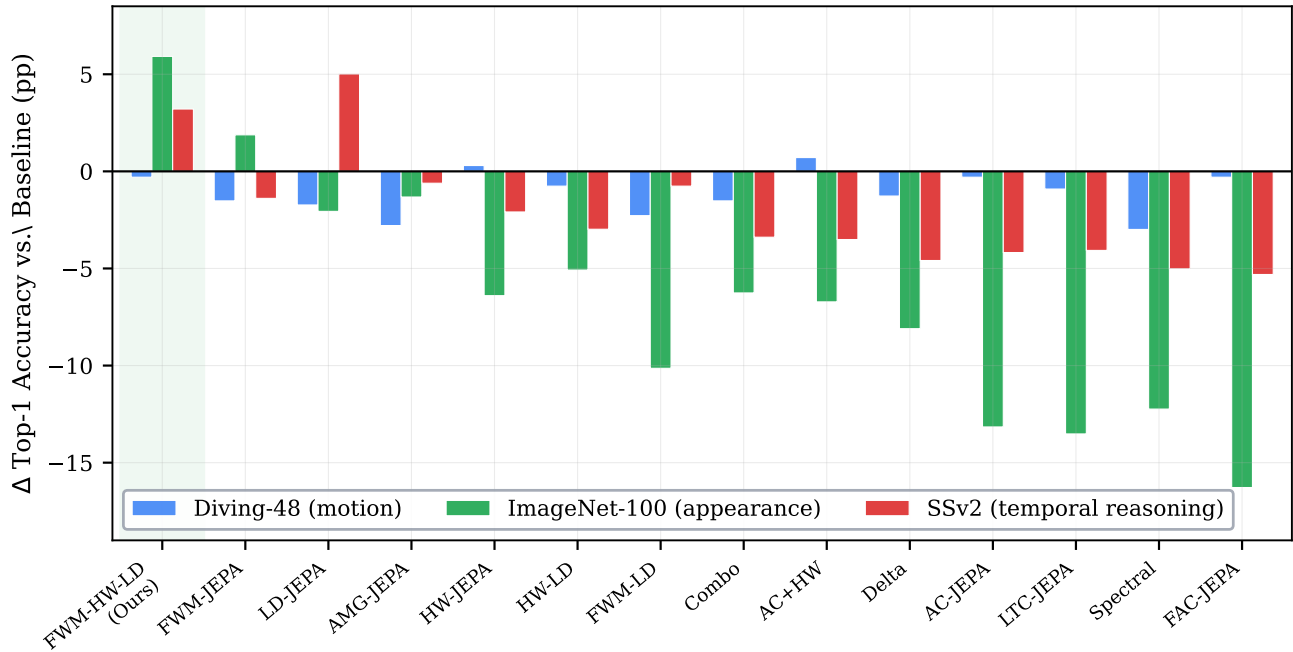


Figure 2. **Capacity trade-offs across mixed-dataset methods.** Grouped bars show percentage-point Δ accuracy relative to baseline on three benchmarks. FWM-HW-LD (leftmost, highlighted) improves appearance (ImageNet-100, green) and temporal reasoning (SSv2, red) while staying close to the Diving-48 baseline. Pixel-prediction methods (AC-JEPA, FAC-JEPA) perform poorly on ImageNet-100 in this setting.

denced by trade-off patterns: kinematic variants gain +1.5–1.7 pp on ImageNet but lose -2.5 – -2.9 pp on Diving-48; action-conditioning variants preserve Diving-48 but substantially degrade appearance.

6.2. Why Factorization May Help

FWM-HW-LD may help by structurally partitioning the latent space during training. Z_{app} is encouraged to remain

Ablation: Components of FWM-HW-LD

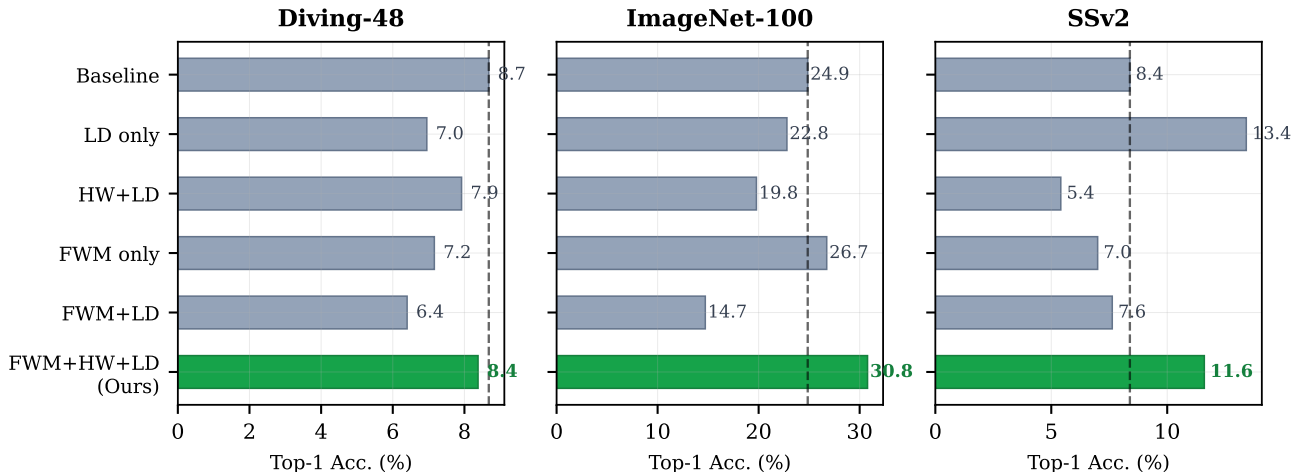


Figure 3. **Ablation of FWM-HW-LD components.** Dashed lines indicate the baseline. The tested components interact non-additively: LD alone boosts SSv2 but hurts others; FWM alone boosts ImageNet-100 modestly; FWM+LD without hard weighting performs poorly on ImageNet-100. The full FWM+HW+LD combination (green bars) gives the most balanced result in this single-seed ablation.

Table 5. Ablation of FWM-HW-LD components on mixed-dataset pretraining. “HW+LD” and “FWM+HW+LD” include both hard-weighted JEPa prediction and hard-weighted latent dynamics.

Components	D-48	IN-100	SSv2
Baseline	8.68	24.86	8.39
LD only	6.95	22.80	13.41
HW + LD	7.92	19.78	5.41
FWM only	7.16	26.74	7.00
FWM + LD	6.40	14.72	7.63
FWM + HW + LD	8.38	30.78	11.60

Table 6. 8-class synthetic motion task (translation, rotation, scaling).

Method	Accuracy (%)
Baseline	27.5
Kinematic-L1 ($\lambda=1.0$)	67.5
Kinematic-L1 ($\lambda=0.1$)	72.5

temporally stable via $\mathcal{L}_{\text{static}}$, while Z_{dyn} receives the latent dynamics prediction signal. The orthogonality constraint discourages the two subspaces from encoding redundant information. This interpretation is consistent with the observed ablation trends, but it should be validated with multi-seed runs and representation analysis.

6.3. Pixel Prediction Is Weak in This Setup

AC-JEPa (−13.16 pp IN-100) and FAC-JEPa (−16.28 pp) perform poorly on ImageNet-100. A plausible explanation is that predicting pixel-level RGB deltas encourages sensitivity to low-level changes that are not useful for frozen se-

mantic recognition. This is consistent with the JEPa motivation for feature-space prediction, though it does not prove that all pixel-space auxiliaries are harmful.

6.4. Hard-Region Weighting as an Empirical Stabilizer

In this ablation, hard-region weighting appears important: without it (FWM+LD), ImageNet drops to 14.72%, while the full method reaches 30.78%. We hypothesize that hard-region weighting changes the balance of gradients by focusing the dynamics loss on tokens where temporal prediction error is highest. This is an empirical observation from this sweep, not yet a mechanistic proof.

7. Discussion

7.1. Practical Observations

- Mixed-data encoders:** FWM-HW-LD is the most balanced variant in our mixed-dataset runs, especially when ImageNet-100 and SSv2 are both important.
- Single-dataset pretraining:** Motion-Guided Masking is a simple low-risk baseline worth testing, since it improves all reported UCF-pretraining metrics in our runs.
- Temporal reasoning priority:** LD-JEPa gives the largest SSv2 gain, but with clear degradation on ImageNet-100 and Diving-48.
- Caution:** Pixel-space prediction objectives (AC-JEPa, FAC-JEPa) and several frequency/contrastive objectives hurt transfer in this implementation.

7.2. Limitations and Threats to Validity

This report should be read as a small-scale empirical study. Mixed-dataset experiments are single-seed, so statistical significance remains unknown. The complete three-benchmark mixed baseline used for deltas is a reference run rather than a same-seed replicate for every auxiliary method; the deltas should therefore be interpreted as empirical signals, not precise confidence intervals. FWM-HW-LD also increases training-time complexity by adding auxiliary losses and a dynamics head, although downstream evaluation still uses the frozen student encoder. Pretraining uses UCF-101 + SSv2 + ImageNet-100 rather than the large-scale data used by V-JEPA 2.x; conclusions concern relative objective behavior under this budget, not parity with large-scale models. Three evaluation benchmarks cannot cover all downstream tasks. Hyperparameters (λ_s , λ_o , λ_d , λ_{hw}) were selected conservatively but not exhaustively tuned per method. Finally, although recent JEPA theory supports the view that auxiliary signals shape which distinctions representations preserve [52], our capacity-trade-off interpretation is based on downstream accuracy patterns; stronger evidence would require multi-seed runs, representation diagnostics, and larger-scale replication.

8. Conclusion

We presented a small-scale empirical study of auxiliary objectives for Video-JEPA, evaluating 18 variants across three complementary benchmarks under two pretraining regimes. Our results suggest that auxiliary objectives often expose a trade-off between appearance and dynamics-sensitive behavior in a shared latent representation.

We studied FWM-HW-LD, a training-time objective that structurally separates the latent space and applies focused latent-space dynamics prediction to hard regions. In our mixed-dataset setting, FWM-HW-LD improves ImageNet-100 by +5.92 and SSv2 by +3.21 percentage points, while remaining within 0.30 percentage points of the Diving-48 baseline.

These results suggest that latent-space organization is a useful direction for future Video-JEPA work, but the present evidence is preliminary. Rather than claiming a solved objective, we view factorized latent dynamics as a controlled way to study how appearance and motion-sensitive information compete or cooperate inside a frozen video representation.

Acknowledgments. I thank the Computer Vision Lab, CAIDAS & IFI, University of Würzburg, Germany, for the research environment and computing support.

References

[1] Anurag Arnab, Mostafa Dehghani, Georg Heigold, Chen Sun, Mario Lučić, and Cordelia Schmid. ViViT: A video

- vision transformer. In *ICCV*, 2021. 2
- [2] Mahmoud Assran, Quentin Duval, Ishan Misra, Piotr Bojanowski, Pascal Vincent, Michael Rabbat, Yann LeCun, and Nicolas Ballas. Self-supervised learning from images with a joint-embedding predictive architecture. In *CVPR*, 2023. 1, 2
- [3] Mahmoud Assran, Adrien Bardes, David Fan, Quentin Garrido, Russell Howes, Mojtaba Komeili, Matthew Muckley, Ammar Rizvi, Claire Roberts, Koustuv Sinha, Artem Zholus, Yann LeCun, Michael Rabbat, and Nicolas Ballas. V-JEPA 2: Self-supervised video models enable understanding, prediction and planning. *arXiv preprint arXiv:2506.09985*, 2025. 1, 2, 5
- [4] Hangbo Bao, Li Dong, Songhao Piao, and Furu Wei. BEiT: Bert pre-training of image transformers. In *ICLR*, 2022. 2
- [5] Adrien Bardes, Jean Ponce, and Yann LeCun. VICReg: Variance-invariance-covariance regularization for self-supervised learning. In *ICLR*, 2022. 2
- [6] Adrien Bardes, Quentin Garrido, Jean Ponce, Xinlei Chen, Michael Rabbat, Yann LeCun, Mahmoud Assran, and Nicolas Ballas. V-JEPA: Video joint embedding predictive architecture. *arXiv preprint arXiv:2404.08471*, 2024. 1, 2, 5
- [7] Gedas Bertasius, Heng Wang, and Lorenzo Torresani. Is space-time attention all you need for video understanding? In *ICML*, 2021. 2
- [8] Mathilde Caron, Ishan Misra, Julien Mairal, Priya Goyal, Piotr Bojanowski, and Armand Joulin. Unsupervised learning of visual features by contrasting cluster assignments. In *NeurIPS*, 2020. 2
- [9] Mathilde Caron, Hugo Touvron, Ishan Misra, Hervé Jégou, Julien Mairal, Piotr Bojanowski, and Armand Joulin. Emerging properties in self-supervised vision transformers. In *ICCV*, 2021. 2
- [10] João Carreira and Andrew Zisserman. Quo vadis, action recognition? a new model and the kinetics dataset. In *CVPR*, 2017. 2
- [11] Ting Chen, Simon Kornblith, Mohammad Norouzi, and Geoffrey Hinton. A simple framework for contrastive learning of visual representations. In *ICML*, 2020. 2
- [12] Xinlei Chen, Haoqi Fan, Ross Girshick, and Kaiming He. Improved baselines with momentum contrastive learning, 2020. 2
- [13] Dima Damen, Hazel Doughty, Giovanni Maria Farinella, Antonino Furnari, Jian Ma, Evangelos Kazakos, Davide Moltisanti, Jonathan Munro, Toby Perrett, Will Price, and Michael Wray. Rescaling egocentric vision: Collection, pipeline and challenges for EPIC-KITCHENS-100. *International Journal of Computer Vision*, 2022. 2
- [14] Carl Doersch, Abhinav Gupta, and Alexei A. Efros. Unsupervised visual representation learning by context prediction. In *ICCV*, 2015. 2
- [15] Alexey Dosovitskiy, Lucas Beyer, Alexander Kolesnikov, Dirk Weissenborn, Xiaohua Zhai, Thomas Unterthiner, Mostafa Dehghani, Matthias Minderer, Georg Heigold, Sylvain Gelly, Jakob Uszkoreit, and Neil Houlsby. An image is worth 16x16 words: Transformers for image recognition at scale. In *ICLR*, 2021. 2, 4

- [16] Haoqi Fan, Bo Xiong, Karttikeya Mangalam, Yanghao Li, Zhicheng Yan, Jitendra Malik, and Christoph Feichtenhofer. Multiscale vision transformers. In *ICCV*, 2021. 2
- [17] Christoph Feichtenhofer, Haoqi Fan, Jitendra Malik, and Kaiming He. Slowfast networks for video recognition. In *ICCV*, 2019. 2
- [18] Christoph Feichtenhofer, Haoqi Fan, Yanghao Li, and Kaiming He. Masked autoencoders as spatiotemporal learners. In *NeurIPS*, 2022. 2
- [19] Raghav Goyal, Samira Ebrahimi Kahou, Vincent Michalski, Joanna Materzynska, Susanne Westphal, Heuna Kim, Valentin Haenel, Ingo Fruend, Peter Yianilos, Moritz Mueller-Freitag, Florian Hoppe, Christian Thureau, Ingo Bax, and Roland Memisevic. The “something something” video database for learning and evaluating visual common sense. In *ICCV*, 2017. 1, 2, 4, 5
- [20] Jean-Bastien Grill, Florian Strub, Florent Althé, Corentin Tallec, Pierre H. Richemond, Elena Buchatskaya, Carl Doersch, Bernardo Avila Pires, Zhaohan Daniel Guo, Mohammad Gheshlaghi Azar, Bilal Piot, Koray Kavukcuoglu, Rémi Munos, and Michal Valko. Bootstrap your own latent: A new approach to self-supervised learning. In *NeurIPS*, 2020. 2
- [21] Agrim Gupta, Lijun Yu, Kihyuk Sohn, Xiuye Gu, Meera Hahn, Fei-Fei Li, Irfan Essa, Lu Jiang, and José Lezama. Siamese masked autoencoders. In *NeurIPS*, 2024. 2
- [22] Tengda Han, Weidi Xie, and Andrew Zisserman. Self-supervised co-training for video representation learning. In *NeurIPS*, 2020. 2, 4
- [23] Kaiming He, Haoqi Fan, Yuxin Wu, Saining Xie, and Ross Girshick. Momentum contrast for unsupervised visual representation learning. In *CVPR*, 2020. 2
- [24] Kaiming He, Xinlei Chen, Saining Xie, Yanghao Li, Piotr Dollár, and Ross Girshick. Masked autoencoders are scalable vision learners. In *CVPR*, 2022. 1, 2, 3
- [25] Irina Higgins, Loic Matthey, Arka Pal, Christopher Burgess, Xavier Glorot, Matthew Botvinick, Shakir Mohamed, and Alexander Lerchner. β -VAE: Learning basic visual concepts with a constrained variational framework. In *ICLR*, 2017. 2
- [26] R Devon Hjelm, Alex Fedorov, Samuel Lavoie-Marchildon, Karan Grewal, Phil Bachman, Adam Trischler, and Yoshua Bengio. Learning deep representations by mutual information estimation and maximization. In *ICLR*, 2019. 2
- [27] Diederik P. Kingma and Max Welling. Auto-encoding variational bayes. In *ICLR*, 2014. 2
- [28] Quan Kong, Wen Wei, Ziwei Deng, Tomoo Yoshinaga, and Tomokazu Murakami. Cycle-contrast for self-supervised video representation learning. In *NeurIPS*, 2020. 2, 4
- [29] Yann LeCun. A path towards autonomous machine intelligence, 2022. Open review essay. 1, 2
- [30] Yingwei Li, Yi Li, and Nuno Vasconcelos. Resound: Towards action recognition without representation bias. In *ECCV*, 2018. 1, 2, 5
- [31] Ze Liu, Jia Ning, Yue Cao, Yixuan Wei, Zheng Zhang, Stephen Lin, and Han Hu. Video swin transformer. In *CVPR*, 2022. 2
- [32] Ilya Loshchilov and Frank Hutter. Decoupled weight decay regularization. In *ICLR*, 2019. 4
- [33] Luc Maes, Quentin Le Lidec, Damien Scieur, Yann LeCun, and Randall Balestriero. LeJEPa: Stable joint-embedding predictive architectures with sketched-isotropic-Gaussian regularization. *arXiv preprint arXiv:2511.08544*, 2025. 1, 2, 3
- [34] Ishan Misra, C. Lawrence Zitnick, and Martial Hebert. Shuffle and learn: Unsupervised learning using temporal order verification. In *ECCV*, 2016. 2
- [35] Lorenzo Mur-Labadia, Matthew Muckley, Amir Bar, Mido Assran, Koustuv Sinha, Mike Rabbat, Yann LeCun, Nicolas Ballas, and Adrien Bardes. V-JEPA 2.1: Unlocking dense features in video self-supervised learning. *arXiv preprint arXiv:2603.14482*, 2026. 2
- [36] Mehdi Noroozi and Paolo Favaro. Unsupervised learning of visual representations by solving jigsaw puzzles. In *ECCV*, 2016. 2
- [37] Aaron van den Oord, Yazhe Li, and Oriol Vinyals. Representation learning with contrastive predictive coding, 2018. 2
- [38] Tian Pan, Yibing Song, Tianyu Yang, Wenhao Jiang, and Wei Liu. Videomoco: Contrastive video representation learning with temporally adversarial examples. In *CVPR*, 2021. 2
- [39] Deepak Pathak, Ross Girshick, Piotr Dollár, Trevor Darrell, and Bharath Hariharan. Learning features by watching objects move. In *CVPR*, 2017. 2, 3
- [40] Adrià Recasens, Pauline Luc, Jean-Baptiste Alayrac, Luyu Wang, Florian Strub, Corentin Tallec, Mateusz Malinowski, Viorica Pătrăucean, Florent Althé, Michal Valko, Jean-Bastien Grill, Aaron van den Oord, and Andrew Zisserman. Broaden Your Views for Self-Supervised Video Learning. In *ICCV*, 2021. 2, 4
- [41] Olga Russakovsky, Jia Deng, Hao Su, Jonathan Krause, Sanjeev Satheesh, Sean Ma, Zhiheng Huang, Andrej Karpathy, Aditya Khosla, Michael Bernstein, Alexander C. Berg, and Li Fei-Fei. ImageNet large scale visual recognition challenge. In *International Journal of Computer Vision*, 2015. 2, 4, 5
- [42] Khurram Soomro, Amir Roshan Zamir, and Mubarak Shah. UCF101: A dataset of 101 human actions classes from videos in the wild. In *CRCV-TR-12-01*, 2012. 2, 4
- [43] Chen Sun, Austin Myers, Carl Vondrick, Kevin Murphy, and Cordelia Schmid. Videobert: A joint model for video and language representation learning. In *ICCV*, 2019. 2
- [44] Yonglong Tian, Dilip Krishnan, and Phillip Isola. Contrastive multiview coding. In *ECCV*, 2020. 2
- [45] Zhan Tong, Yibing Song, Jue Wang, and Limin Wang. VideoMAE: Masked autoencoders are data-efficient learners for self-supervised video pre-training. In *NeurIPS*, 2022. 1, 2, 3
- [46] Du Tran, Heng Wang, Lorenzo Torresani, Jamie Ray, Yann LeCun, and Manohar Paluri. A closer look at spatiotemporal convolutions for action recognition. In *CVPR*, 2018. 2
- [47] Ashish Vaswani, Noam Shazeer, Niki Parmar, Jakob Uszkoreit, Llion Jones, Aidan N. Gomez, Lukasz Kaiser, and Illia Polosukhin. Attention is all you need. In *NeurIPS*, 2017. 2
- [48] Limin Wang, Bingkun Huang, Zhiyu Zhao, Zhan Tong, Yinan He, Yi Wang, Yali Wang, and Yu Qiao. VideoMAE V2:

- Scaling video masked autoencoders with dual masking. In *CVPR*, 2023. [2](#)
- [49] Zhenda Xie, Zheng Zhang, Yue Cao, Yutong Lin, Jianmin Bao, Zhuliang Yao, Qi Dai, and Han Hu. SimMIM: A simple framework for masked image modeling. In *CVPR*, 2022. [2](#)
- [50] Dejing Xu, Jun Xiao, Zhou Zhao, Jian Shao, Di Xie, and Yueting Zhuang. Self-supervised spatiotemporal learning via video clip order prediction. In *CVPR*, 2019. [2](#)
- [51] Shen Yan, Xuehan Xiong, Anurag Arnab, Zhicheng Lu, Mi Zhang, Chen Sun, and Cordelia Schmid. Video representation learning using discriminative pooling. In *CVPR*, 2022. [2](#)
- [52] Jiacan Yu, Siyi Chen, Mingrui Liu, Nono Horiuchi, Vladimir Braverman, Zicheng Xu, Dan Haramati, and Randall Balestriero. Why and how auxiliary tasks improve JEPA representations. *arXiv preprint arXiv:2509.12249*, 2025. [1](#), [2](#), [8](#)
- [53] Jure Zbontar, Li Jing, Ishan Misra, Yann LeCun, and Stéphane Deny. Barlow twins: Self-supervised learning via redundancy reduction. In *ICML*, 2021. [2](#)

A. Pseudocode for Key Methods

Algorithm 1 summarizes the standard V-JEPA training loop. Algorithm 2 describes FWM-HW-LD, which extends the baseline with hard-weighted prediction, factorization losses, and hard-weighted latent dynamics.

Algorithm 1 Baseline V-JEPA Training

Require: Video clip x , random mask m

- 1: $z_{\text{vis}} \leftarrow f_{\theta}(x, \text{visible} = \bar{m})$
 - 2: $\hat{z} \leftarrow g_{\phi}(z_{\text{vis}}, m)$
 - 3: $h \leftarrow \text{sg}(f_{\hat{\theta}}(x))$
 - 4: $\mathcal{L} \leftarrow \|\hat{z} - h[m]\|_1$
 - 5: Update f_{θ}, g_{ϕ} via backprop
 - 6: EMA: $\theta \leftarrow 0.99925 \cdot \theta + 0.00075 \cdot \theta$
-

Algorithm 2 FWM-HW-LD Training (Eq. 12)

Require: Video clip x , mask m , ratios $D_{\text{app}}=D/2$

- 1: Compute JEPA loss $\mathcal{L}_{\text{JEPA}}$ (Algorithm 1)
 - 2: $e_i^{\text{jepa}} \leftarrow \|\hat{z}_i - h_i[m]\|_1$
 - 3: $w_i^{\text{jepa}} \leftarrow \text{softmax}(e_i^{\text{jepa}}/\tau) \cdot N_{\text{tok}}$
 - 4: $\mathcal{L}_{\text{HW-JEPA}} \leftarrow \text{mean}(w_i^{\text{jepa}} \cdot e_i^{\text{jepa}})$
 - 5: $z \leftarrow f_{\theta}(x), h \leftarrow \text{sg}(f_{\hat{\theta}}(x))$
 - 6: $Z_{\text{app}}, Z_{\text{dyn}} \leftarrow z[\dots, :D_{\text{app}}], z[\dots, D_{\text{app}}:]$
 - 7: $\mathcal{L}_{\text{static}} \leftarrow \text{mean}(\|Z_{\text{app}}^{(t+1)} - Z_{\text{app}}^{(t)}\|)$
 - 8: $\mathcal{L}_{\text{orth}} \leftarrow \|C_{Z_{\text{app}}}^T C_{Z_{\text{dyn}}}\|_F^2 / N$
 - 9: $\hat{\Delta} \leftarrow \text{DynHead}(Z_{\text{dyn}}^{(t)})$
 - 10: $\Delta h \leftarrow h^{(t+1)} - h^{(t)}$
 - 11: $e_i \leftarrow \|\hat{\Delta}_i - \Delta h_i\|_1$ {per-token error}
 - 12: $w_i^{\text{ld}} \leftarrow \text{softmax}(e_i/\tau) \cdot N_{\text{tok}}$ {hard-region weights}
 - 13: $\mathcal{L}_{\text{LD-HW}} \leftarrow \text{mean}(w_i^{\text{ld}} \cdot e_i)$
 - 14: $\mathcal{L} \leftarrow \mathcal{L}_{\text{JEPA}} + \lambda_{hw}\mathcal{L}_{\text{HW-JEPA}} + \lambda_s\mathcal{L}_{\text{static}} + \lambda_o\mathcal{L}_{\text{orth}} + \lambda_d\mathcal{L}_{\text{LD-HW}}$
-

The dynamics head `DynHead` is a two-layer MLP with hidden dimension 256 and GELU activation. When FWM is active, the input dimension is reduced to $D_{\text{dyn}} = D - D_{\text{app}}$ to ensure that dynamics prediction does not draw on appearance features.

B. Hyperparameters

Table 7 lists all hyperparameters across the 18 method variants. We did not perform per-method hyperparameter tuning; values were chosen based on small-scale preliminary runs and held fixed across all main experiments to ensure fair comparison. Coefficients λ_s and λ_o for FWM are deliberately small to act as regularizers rather than dominant objectives, while λ_d is unit weight to provide a meaningful learning signal for the dynamics head. The HW temperature τ controls the sharpness of hard-region weighting; $\tau = 1$

provides a soft attention over the per-token error distribution.

Table 7. Hyperparameters for all auxiliary objectives.

Parameter	Used by	Value
λ_{kin}	Kinematic variants	0.1 or 1.0
λ_s (static)	FWM variants	0.05
λ_o (orth.)	FWM variants	0.01
D_{app}/D	FWM variants	0.5
λ_d (LD)	LD variants	1.0
LD hidden dim	LD variants	256
HW temperature τ	HW variants	1.0
λ_{HW}	HW, AC+HW, Combo / HW-LD, FWM-HW-LD	0.3 / 1.0
λ_{AC}	AC, AC+HW, FAC	1.0
λ_{Δ} (delta)	Delta-JEPA, Combo	0.5
λ_{spec}	Spectral-JEPA	1.0
$\lambda_{\text{LTC}} / \text{margin}$	LTC-JEPA	0.5 / 0.5
Motion fallback rate	Motion-Guided / AMG	0.1 / 0.0

C. Computational Resources

All experiments were conducted on a Kubernetes cluster with NVIDIA A100 GPUs (40 GB). Each pretraining run uses 4 GPUs with global batch size 32 for 100 epochs of 300 iterations each, completing in approximately 7 hours. Frozen-encoder evaluation runs require an additional 2–6 hours per benchmark, depending on dataset size. Table 8 summarizes the total budget.

Table 8. Computational budget for the full study.

Resource	Value
GPUs per training run	4 × NVIDIA A100 (40 GB)
Training time per run	~7 hours
Number of training runs	18
Total pretraining GPU-h	~504 GPU-h
Eval runs per method	3 (D-48, IN-100, SSv2)
Eval time per benchmark	~2–6 hours
Total evaluation GPU-h	~720 GPU-h
<hr/>	
Total compute	~1,224 GPU-h
Backbone	ViT-Base (86M parameters)
Framework	PyTorch, distributed (DDP)

D. Additional Implementation Notes

Mixed-data sampling. For mixed-dataset pretraining, we sample batches with weights 20% UCF-101, 60% SSv2, and 20% ImageNet-100. Image samples from ImageNet-100 are converted to single-frame “videos” (tubelet length 1) so that the same data pipeline handles all three sources. The 60% SSv2 weight reflects our explicit goal of strengthening temporal reasoning.

Mask sampling. The default V-JEPA mask is a multi-block spatiotemporal tube. For Motion-Guided Masking, we compute per-frame motion energy as the mean L1 difference between consecutive frames at the patch level, nor-

malize per-clip, and sample mask centers proportional to the resulting score. With probability 0.1 we fall back to uniform random sampling to retain coverage of static regions.

Latent dynamics head input. Under FWM-HW-LD, the dynamics head receives only the $D_{\text{dyn}} = D - D_{\text{app}}$ dynamic channels of the student representation; this is implemented by a tensor slice prior to the linear projection. Removing this slice (i.e., letting the dynamics head see the full D -dimensional representation) recovers the LD-JEPA baseline and substantially weakens appearance preservation.

Numerical stability. The hard-region weighting softmax operates on per-token L1 errors that can vary by orders of magnitude across batches. We clip the temperature-scaled logits to $[-20, 20]$ before the softmax to prevent numerical overflow, and we detach the weights from the autograd graph (`torch.no_grad`) so that gradients flow only through the unweighted error.